Elsevier Editorial System(tm) for Clinical Neurophysiology
Manuscript Draft

Manuscript Number:

Title: Removing muscle and eye artifacts using blind source separation techniques in ictal EEG source imaging

Article Type: Full Length Article

Keywords: ictal SPECT; artifact removal; EEG source localization

Corresponding Author: ir Hans Hallez, MScECS

Corresponding Author's Institution: Ghent University

First Author: Hans Hallez

Order of Authors: Hans Hallez; Maarten De Vos; Bart Vanrumste, PhD; Peter Van Hese; Sara Assecondi; Koen Van Laere, PhD, MD; Patrick Dupont, PhD; Wim Van Paesschen, PhD, MD; Sabine Van Huffel, PhD; Ignace Lemahieu, PhD

Suggested Reviewers: Pierre Cluitmans
P.J.M.Cluitmans@tue.nl

Andre Palmini
apalmini@uol.com.br

Opposed Reviewers:

Removing muscle and eye artifacts using blind source separation techniques in ictal EEG source imaging

H. Hallez [a,*], M. De Vos [b], B. Vanrumste [c], P. Van Hese [a], S. Assecondi [a], K. Van Laere [e], P. Dupont [f], W. Van Paesschen [d], S. Van Huffel [b], I. Lemahieu [a],

[a] *MEDISIP - IBBT, Departement of Electronics and Information Systems, Ghent University Hospital - IBITECH, De Pintelaan 185, 9000 Ghent, Belgium*

[b] *Department of Electrical Engineering (ESAT), Kasteelpark Arenberg 10, Leuven, Belgium*

[c] *MOBILAB, Biosciences and Technology Department, Katholieke Hogeschool Kempen, Kleinhoefstraat 4, B-2440 Geel, Belgium*

[d] *Department of Neurology, Division of Experimental Neurology, University Hospital Gasthuisberg, Herestraat 49, 3000 Leuven, Belgium*

[e] *Department of Medical Diagnostic Sciences, Division of Nuclear Medicine, University Hospital Gasthuisberg, E901, Herestraat 49, 3000 Leuven, Belgium*

[f] *Department of Medical Diagnostic Sciences, Laboratory for Cognitive Neurology, University Hospital Gasthuisberg, Herestraat 49, 3000 Leuven, Belgium*

Abstract

Objective: The contamination of muscle and eye artifacts during an ictal period of the EEG greatly distorts source estimation algorithms. Recent blind source separation (BSS) techniques based on canonical correlation (BSS-CCA) and independent components analysis with spatial constraints (SCICA) have shown much promise in the removal of these artifacts. In this study we want to use BSS-CCA and SCICA as a preprocessing step before the source estimation during the ictal period.

Methods: Both the contaminated and cleaned ictal EEG are subjected to the RAP-MUSIC algorithm. This is a multiple dipole source estimation technique based on the separation of the EEG in a signal and noise subspace. Although the subtracted ictal SPECT (iSPECT) coregistered to magnetic resonance image (SISCOM) images the ictal onset zone with a propagation, they were used to compare the source estimations with. Both sets of source estimations from the contaminated and cleaned EEG were correlated with the ictal SPECT by measuring the distance between the dipoles and the iSPECT activation during the start of the seizure.

Results: We applied the artifact removal and the source estimation on 8 patients. Qualitatively, we can see that in 6 out of 8 patients show an improvement of the

dipoles. The dipoles are nearer to or have tighter clusters near the iSPECT activation. From the median of the distance measure, we could appreciate that 5 out of 8 patients show improvement.

Conclusions: The results show that BSS-CCA and SCICA can be applied to remove artifacts, but the results should be interpreted with care. The results of the source estimation can be misleading due to excessive noise or modeling errors. Therefore, the accuracy of the source estimation can be increased by incorporating other imaging modalities like ictal SPECT.

Significance: This is a pilot study where the diagnosis of epilepsy can be made more reliable if multiple modalities are combined.

Key words: ictal SPECT, artifact removal, EEG source localization
PACS: 87.85.-d, 87.85.Ng, 87.85.Pq

---

* Corresponding author. address: Ghent University Hospital - IBITECH, De Pintelaan 185, 9000 Ghent, Belgium.
Email address: hans.hallez@UGent.be (H. Hallez).

* Manuscript

Removing muscle and eye artifacts using blind source separation techniques in ictal EEG source imaging

H. Hallez [a,*], M. De Vos [b], B. Vanrumste [c], P. Van Hese [a], S. Assecondi [a], K. Van Laere [e], P. Dupont [f], W. Van Paesschen [d], S. Van Huffel [b], I. Lemahieu [a],

[a] *MEDISIP - IBBT, Departement of Electronics and Information Systems, Ghent University Hospital - IBITECH, De Pintelaan 185, 9000 Ghent, Belgium*

[b] *Department of Electrical Engineering (ESAT), Kasteelpark Arenberg 10, Leuven, Belgium*

[c] *MOBILAB, Biosciences and Technology Department, Katholieke Hogeschool Kempen, Kleinhoefstraat 4, B-2440 Geel, Belgium*

[d] *Department of Neurology, Division of Experimental Neurology, University Hospital Gasthuisberg, Herestraat 49, 3000 Leuven, Belgium*

[e] *Department of Medical Diagnostic Sciences, Division of Nuclear Medicine, University Hospital Gasthuisberg, E901, Herestraat 49, 3000 Leuven, Belgium*

[f] *Department of Medical Diagnostic Sciences, Laboratory for Cognitive Neurology, University Hospital Gasthuisberg, Herestraat 49, 3000 Leuven, Belgium*

Abstract

Objective: The contamination of muscle and eye artifacts during an ictal period of the EEG greatly distorts source estimation algorithms. Recent blind source separation (BSS) techniques based on canonical correlation (BSS-CCA) and independent components analysis with spatial constraints (SCICA) have shown much promise in the removal of these artifacts. In this study we want to use BSS-CCA and SCICA as a preprocessing step before the source estimation during the ictal period.

Methods: Both the contaminated and cleaned ictal EEG are subjected to the RAP-MUSIC algorithm. This is a multiple dipole source estimation technique based on the separation of the EEG in a signal and noise subspace. Although the subtracted ictal SPECT (iSPECT) coregistered to magnetic resonance image (SISCOM) images the ictal onset zone with a propagation, they were used to compare the source estimations with. Both sets of source estimations from the contaminated and cleaned EEG were correlated with the ictal SPECT by measuring the distance between the dipoles and the iSPECT activation during the start of the seizure.

Results: We applied the artifact removal and the source estimation on 8 patients. Qualitatively, we can see that in 6 out of 8 patients show an improvement of the

dipoles. The dipoles are nearer to or have tighter clusters near the iSPECT activation. From the median of the distance measure, we could appreciate that 5 out of 8 patients show improvement.

Conclusions: The results show that BSS-CCA and SCICA can be applied to remove artifacts, but the results should be interpreted with care. The results of the source estimation can be misleading due to excessive noise or modeling errors. Therefore, the accuracy of the source estimation can be increased by incorporating other imaging modalities like ictal SPECT.

Significance: This is a pilot study where the diagnosis of epilepsy can be made more reliable if multiple modalities are combined.

Key words: ictal SPECT, artifact removal, EEG source localization
PACS: 87.85.-d, 87.85.Ng, 87.85.Pq

1 Introduction

Epilepsy is a neurological disorder caused by spontaneous rhythmic electrical activity of groups of neurons. The manifestion of such activity is called an epileptic seizure. Often, the disorder can be treated with medication. In 30% of the cases, however, patients develop drug-resistant epilepsy. These patients can sometimes be helped by resecting the origin of the epileptic seizure (the so-called epileptogenic focus) with a surgical operation. A presurgical evaluation has to be performed in order to determine an accurate location of the epileptogenic focus (Boon et al., 1999).

In the last decade different methods have been developed to estimate the location of the intracranial source of the epileptic activity from the scalp-EEG. Dipole sources are an adequate model that are used very often to represent focal epileptic activity. These dipole sources have 3 spatial coordinates and 3 components and can be estimated by EEG dipole analysis (Baillet et al., 2001). Therefore, the EEG dipole source analysis is a useful tool in the presurgical evaluation in ictal EEG (Boon et al., 2002; Sakai et al., 2002) as well as interictal EEG (Ding et al., 2006).

Another useful technique used in the presurgical evaluation to determine the ictal onset zone is SISCOM (subtracted ictal SPECT coregistered on MRI) (Van Paesschen, 2004; Lee et al., 2006). Specifically, single photon emission computed tomography (SPECT) provides a 3D distribution of the activity in

* Corresponding author. address: Ghent University Hospital - IBITECH, De Pintelaan 185, 9000 Ghent, Belgium.
Email address: hans.hallez@UGent.be (H. Hallez).

the brain. In clinical practice, this technique can be used to image the location of the epileptogenic focus.

Both techniques have benefits and culprits. The time resolution of the perfusion SPECT is in the order of 30-60 seconds and thus very low. In contrast, the EEG is a direct reflection of the electrophysiological activity, which results in a high temporal resolution (order of milliseconds).

Regarding spatial resolution, SPECT (5-10 mm) outperforms the source analysis of the EEG (2 - 4 cm). The estimation of sources from ictal EEG is often distorted by non-cerebral activity. During a epileptic seizure, muscle activity is very prominent and is reflected in the EEG by a high frequent random signal. Localizing the source during an episode with muscle activity will most likely result in a source close to the muscles (Niedermeyer and Lopez Da Silva, 2004; Stern and Engel, 2004). Low-pass filters are commonly used to remove muscle artifacts. However, as the frequency spectrum of muscle artifacts overlaps with that of interesting brain signals (Goncharova et al., 2003), also valuable information in the EEG concerning brain activity is removed when applying low-pass filters.

Eye blink and eye movement artifacts are other sources of non-cerebral activity which can distort the EEG. These artifacts are caused by closing and opening of the eyes and are most prominent is the electrodes placed near the eyes. The characteristics are low frequent, non-stationary and high amplitude (Niedermeyer and Lopez Da Silva, 2004; Stern and Engel, 2004).

Blind source separation (BSS) techniques, like independent component analysis (ICA), have shown promising results in the field of artifact removal (Choi et al., 2005; Nam et al., 2002). De Clercq et al. used a BSS technique based on canonical correlation analysis (CCA), which assumes mutually uncorrelated sources which are maximally autocorrelated. Muscle sources indeed have a low autocorrelation with respect to brain activity (De Clercq et al., 2006; Friman et al., 2002). For the removal of eye-artifacts several techniques have been proposed. However, most of them require the availability of peri-ocular electro-oculographic (EOG) electrodes (Joyce et al., 2004; Jung et al., 2000; Shoker et al., 2005). These EOG electrodes are not always recorded as they are too cumbersome for the patient. Li et al. developed an ICA-based technique without the need of EOG channels, but this technique is limited to remove eye blinks and not eye movements (Li et al., 2006). De Vos et al. used an spatially constrained ICA technique (SCICA) to remove eye blinks and movements (De Vos et al., 2006a).

In Lantz et al. (1999) the authors investigated the dominant frequencies due to ictal activity. Their study showed that the dominant frequency during an epileptic seizure shifted within the range of 3.5 and 8.5 Hz over time. However,

their analysis excluded artifactuated epochs. Assaf and Ebersole (1997) used a very narrow bandpass filters (between 2 and 20 Hz) to remove the muscle and movement artifacts in order to obtain a signal with high signal-to-noise ratio. They showed that the source estimation correlated well with the temporal seizure onset zone. However, it is well known that the EEG ranges within the 0.5 to 45 Hz. Hence, the application of narrow band filters will filter out valuable information from the EEG.

In this study we applied BSS-CCA (De Clercq et al., 2006) and SCICA (De Vos et al., 2006a) as a preprocessing step to remove artifacts for source analysis of EEG, contaminated with muscle and eye movement artifacts. In this way, we wanted to improve the localization of the sources originating from ictal epileptic activity.

2 Materials

The EEG was measured in a clinical setup at the Universitary hospital U.Z. Gasthuisberg in Leuven, Belgium. The electrodes were placed in a 10-20 standard system with 2 extra temporal electrodes and the sample rate was 250 Hz. The EEG fragments were about 2 minutes in length and the start of the seizure was indicated by an experienced neurologist. From eight patients where the SISCOM revealed the focus which was visually inspected by the neurologist, the EEG fragments were collected and processed using MATLAB. Information about the patients used in this study is shown in table 1.

3 Methods

3.1 Removing muscle and eye movement artifacts by Blind Source Separation (BSS) techniques

The EEG measures the sum of all electrical activity, synchronous neuronal firing and electrical artifacts. As these artifacts disturb accurate localisation, they have to be removed first. The goal of independent component analysis (ICA) is to extract from a linear mixture of independent sources the source signals.

Mathematically, assume the basic linear statistical model

$$Y = \mathbf{M} \cdot X + N \tag{1}$$

where $Y \in \mathbb{R}^I$ is called the observation vector (I is the number of observation channels), $X \in \mathbb{R}^J$ the source vector (J is the number of sources) and $N \in \mathbb{R}^I$ additive noise. $\mathbf{M} \in \mathbb{R}^{I \times J}$ is the mixing matrix.

The goal of Independent Component Analysis is to estimate the mixing matrix $\mathbf{M}$, and/or the source vector X, given only realizations of Y. In this study, we assume that $I \geqslant J$.
Blind identification of $\mathbf{M}$ in (1) is only possible when some assumptions about the sources are made.

One assumption is that the sources are mutually statistically independent, as well as independent from the noise components and that at most one source is gaussian (Comon, 1994).

Another assumption is that the sources are mutually uncorrelated but individually correlated in time. Under these assumptions, the sources can be estimated with the SOBI algorithm (Belouchrani et al., 1997). This algorithm has shown to be useful in several biomedical applications. The SOBI algorithm is based on second order statistics. This reduces the need for having long measurements of the observation signal as it is the case when higher order statistics are computed (e.g. in Comon (1994)) before computing the source signals. This is necessary for the on-line application under investigation.
Eye artifacts are highly correlated in time and can be separated with SOBI from background EEG. With the standard SOBI algorithm, the sources corresponding to eye artifacts have to be selected after the decomposition. However, the prior knowledge on the spatial distribution can be exploited to decompose the EEG with the constrained algorithm SCICA (De Vos et al., 2006b).

Yet another possible assumption is that the sources are individually correlated in time and that all sources have a different autocorrelation. In this case an algorithm based Canonical Correlation Analysis (CCA) (Hotelling, 1936) can be used to recover the source signals. Muscle artifacts are characterised by a much lower autocorrelation than background EEG. So this algorithm can be used to extract and remove muscle artifacts.

3.2 Estimating the sources by RAP-MUSIC

When the muscle and eye artifacts are removed, one can search for the dipole sources. The EEG dipole localization problem is twofold. First, the forward states the relations between the potential values at the scalp electrodes and a given source. The electrode potentials are obtained by solving Poisson's equation given a dipole source in a specified geometry. The head model we used, was a realistic head model derived from an T1 Magnetic Resonance

scan. The head model was segmented in 4 compartments: scalp tissue, skull, cerebrospinal fluid (CSF) and brain tissue. The head model was then placed into a cubic calculation grid, where the inter node distance was 1 mm. The conductivities of the compartments were isotropic and were equal 0.33 S/m, 0.020 S/m, 1 S/m and 0.33 S/m for scalp tissue, skull, CSF and brain tissue respectively (Ferree et al., 2000; Gonçalves et al., 2003). The 21 electrode positions were set in a standard 10-20 system and were hence not adjusted to the patient specific positions. The forward problem was then solved by using an finite difference method (Hallez et al., 2005).

Second, the inverse problem searches parameters of the dipole given the scalp potentials. A number of methods have been developed to estimate the dipolar source, depending on the assumptions of the input EEG potentials. In this study we used a multidipolar estimation technique, i.e. RAP-MUSIC (Mosher and Leahy, 1999). This assumes that the topographies due to the dipole sources are orthogonal (uncorrelatedness) and that the topographies are sorted by energy in the EEG fragment.

The relative residual energy is a measure of the "goodness-of-fit" and is defined as the relative amount of energy in the EEG that cannot be explained by the p dipoles, found by the RAP-MUSIC algorithm:

$$RRE = \frac{\|(\sum_i^p \mathbf{G}(\mathbf{r}_i, \mathbf{d_i})) - \mathbf{V}\|}{\|\mathbf{V}\|} \tag{2}$$

where $\mathbf{G}(\mathbf{r}_i, \mathbf{d}_i)$ are the scalp potentials caused by the i-th dipole at location $\mathbf{r}_i$ and orientation $\mathbf{d}_i$. The electrode potentials can obtained by solving the forward problem.

In the dipole estimation using RAP-MUSIC, the number of estimated dipoles in this study was limited to 2. The reason for this was that it sometimes occurred that the dipoles were modeling pure noise and tried to represent very low potentials at the electrodes. The result is that one obtaines dipole estimations that have a high magnitude but cancel each other out. In the case of 2 dipoles, one can restrict the dipole estimation in such way that the location of the 2 dipole estimations should be farther than 1 cm apart, as was done in this paper. For a higher number of dipole estimations, more complex restriction rules should be used.

3.3 Fusing the EEG dipole source estimations and SPECT activity

It is known that ictal SPECT activity has a better spatial resolution and a low temporal resolution, compared to the EEG dipole estimations which have

a high temporal resolutions, but moderate spatial resolutions. By combining the ictal SPECT activity with the dipole estimations from the RAP-MUSIC algorithm, we can evaluate the proximity of the dipole estimations before and after the artifact removal. Therefore we want to compare the EEG dipole estimations with the SPECT activations, which depicts the ictal onset zone with a propagation of the activity to other area's.

The SPECT image of the SISCOM was normalized and a 95% threshold was set, considering only the activity above that threshold. We assumed that the edge of the 95% surface confined the seizure onset zone. These confinements are shown in figures 4, 5, 6 and 7 as red blobs. Note that the activity delineated by the 95% surface could also be multifocal. In that case, the epileptic seizure was already propagated into other regions.

The concurrence between the EEG dipole analysis and SPECT activity can then be measured with the distance between the dipoles estimated from the RAP-MUSIC and the edge of the SPECT activation (see figure 1). The smaller the distance measure, the closer the dipoles are to the SPECT activation of the epileptogenic onset zone.

3.4 Experimental setup

Starting from the EEG fragment of two minutes, the EEG was processed using the CCA and the SCICA algorithms to filter out the muscle and eye blink artifacts. For each patient we obtained a raw and a filtered EEG. Both the filtered and unfiltered EEG fragments were processed by RAP-MUSIC. The seizure onset on the EEG was depicted by a neurologist. The source estimations was done in moving windows from 1 second before the seizure onset to 20 seconds after the seizure onset. In this way we want to compensate for the difference in timing of the dipole estimations and the EEG dipole source estimations.

RAP-MUSIC was applied in moving windows of 62 samples (~ 0.25 ms) with step size 6 samples (~ 0.025 ms)). In each window a maximum of 2 dipoles were estimated using the scanning procedure, with the minimum requirement that the correlation between the topography of the dipole sources and the signal subspace was at least 95%. This yields sources that are dominant in the EEG. If one of the sources did not meet the requirements, only one dipole was estimated.

When used in a moving window the RRE can be seen as a goodness-of-fit in function of time. To identify focal sources, we selected the dipole estimations that resulted in an RRE within the first quantile of the total set of RREs in the 21 second time window. In this way we selected the sources that gave the

best goodness-of-fit as the goodness-of-fit is dependent for each patient and the noise in the EEG. Hence, in Hallez et al. (2007) it was shown that the RRE increased when filtering the EEG.

The Euclidean distance from the dipole location to the edge the ictal onset zone indicated by the SPECT was calculated in each moving window. The result is a set of Euclidean distances for each of the at maximum 2 dipoles in that window. These distances were set in function of time and can be correlated with the temporal dimension with the EEG.

3.5 Comparing the distances of the dipoles

The result of the dipole estimation is a set of dipole positions and orientation over a time period of 21 seconds (between 1 second before and 20 second after the indicated start of the seizure). The distances with respect to the SPECT activations of the estimated dipoles during that time period are calculated illustrated in 1. To exclude outliers from the measure, we have compared the median distance of the unfiltered with the filtered data.

4 Results

4.1 Examples of artifact removal

In figure 2 and 3 examples are shown of the unfiltered and filtered EEG. Below each EEG fragment, the distances of the dipoles to the thresholded ictal SPECT region is shown. An EEG fragment contaminated with mainly muscle artifact is shown in figure 2a. Below this figure the distance of the dipoles to the center of gravity of the SPECT activation is shown. At most two distances per window are calculated. The black asterisk and blue asterisk indicate the distance of the first and second dipole to the ictal SPECT activation, respectively. We can see that the distance has a high variability. The dipole estimations show no clusters and a lot of dipoles are estimated at the edge of the brain compartment. Applying the muscle and eye artifact removal techniques results in the EEG shown in 2b. We can appreciate from the figures that the EEG muscle artifact has been reduced. As seen below the EEG fragment, the distance measure is lower than in the one in the unfiltered EEG fragment. The dipole estimates from this data set are shown in figure 5, patient 3.

To illustrate the filtering of eye blink artefacts, figure 3a and 3b show the

EEG and the distance between the estimated dipoles and the edge of the ictal SPECT activation. Figure 3a show the results in the unfiltered case. While the ictal onset zone is located in the occipital area of the brain, the dipoles are located in the frontal area due to the eye blink artifacts (see figure 7,patient 8). When the eye blink artifacts are removed, the dipoles are located in the occipital area. In the vicinity of the start of the EEG seizure the dipoles were estimated within the enclosed surface of SPECT activity, normalized and thresholded at 95%. This example shows that the filtering of the eye blink artefacts can improve the dipole estimation. Therefore, the distance measure is very high (> 100 mm)at the start of the seizure.

4.2 Estimation of the dipoles in the realistic head model

Figures 4-7 shows the dipole estimations during the 21 second interval (1 second prior to seizure onset till 20 seconds after) of the unfilterd EEG and filtered EEG for different patients. The red blob indicates the contours of the ictal spect activity. In the figures, regions of interest are marked in green. Next, we will go over the results of each individual patient.

For patient 1, 6, 7 and 8 (see figures 4, 5, 6 and 7) we can see that the filtering resulted in tighter clusters near the ictal SPECT activation: in patient 1 and 8 we see that the dipole estimation is distorted by the eye artifacts, as the dipole estimations in the unfiltered data are mainly situated in the front of the head, marked by the region of interest (ROI) in green. After filtering, the activity in the front of the head of patient 1 and 8 was removed successfully. This resulted in more tight cluster in patient 1 in the left temporal lobe very close near the ictal SPECT activation. Patient 8 showed a significant improvement when the eye and muscle artifacts are removed. This resulted in a cluster in the parietal lobe which overlapped with the ictal spect.

Whereas in patient 7 (see figure 7), muscle activity distorts the dipole estimation in the unfiltered data. This is reflected in the dipole estimation of the data as dipole sources in the right parieto-temporal region, marked by the ROI in green. The dipole estimations due to the muscle activity in patient 7 are almost completely removed in the filtered data. We see that the estimated dipole sources during the ictal episode are more frontally situated, near the ictal SPECT regions.

Patient 6 (see figure 6) had a electrode artifact in the EEG. This is clearly visible in the dipole estimations of the unfiltered data. After filtering, the electrode artifact is still present (indicated by the green ROI in both unfiltered and filtered dipole estimations). In the right parietal region, some muscle activity is present in the dipole estimation of the unfiltered EEG, although after

applying the muscle and eye blink removal artifact, the muscle activity was still present. This is marked in the dipole estimates by a magenta ROI.

In patient 3 (see figure 5) and 5 (see figure 6) the filtering revealed new source estimation clusters. Both the EEG fragments of patients 3 and 5 were distorted with muscle activity. Patient 3 is a good example of the usefulness of removing muscle activity prior to source imaging. The muscle activity was mainly situated at the bilateral temporal regions. In this case, the muscle and eye artifact removal revealed new dipole clusters. These clusters show a good agreement with the ictal spect activity at the left temporal region. As in patient 3, patient 5 showed muscle activity at the temporal regions, indicated by the green ROIs in the dipole estimation of the unfiltered EEG. Also dipoles estimations were very diffuse. After applying the artefact removal techniques, the dipole estimation revealed two very tight clusters. Although it is not clear from the figure, several dipole estimations had nearly the same location en orientation.

Patient 2 and 4 did not show a good agreement with the ictal SPECT and the dipole estimation after applying artifact removal. In the case of patient 2 the ictal activity and the muscle activity contained the same spatial information. Thus removing the muscle activity, also removed components related to the ictal activity.

4.3 Comparing the distances

In figure 8 the median distance over the distances of the dipole estimates to the ictal spect in the 21 second windows is shown for each patient in the unfiltered and filtered case.

5 Discussion

Ictal EEG is mostly contaminated with muscle and eye artifacts. This disturbs automatic source localization methods. We used blind source separation techniques (BSS-CCA and SCICA) to remove these artifacts to obtain a better localization of the epileptogenic focus during ictal activity. In this small pilot study, we examined 8 patients suffering from epilepsy.

After applying the muscle and eye blink artifact removal in patient 6 we saw that there is still some residual muscle activity. From the dipole estimates (see figure 6), we can see that there is an electrode artifact in the unfiltered EEG. As an electrode artifact is only visible at one electrode, the other channels are

capable to depict the ictal onset zone. Therefore, the expert did not have to remove the artifactuated channels completely to make the ictal activity visible in the EEG. This fact also holds remaining muscle activity of filtered EEG. Indeed, the muscle activity and ictal activity are situated at very distinct places. The muscle artifact removal of the EEG was not complete, as the ictal activity was already made visible for the expert and hence he did not further remove more muscle artifact components from the CCA. Note that the increase in the number of dipoles is due to the fact that the RRE is not a fixed threshold but is set to select the most focal dipoles by means of the statistics of the RRE over the whole 21 second period. Nevertheless, the removal of the muscle activity did result in a more concentrated cluster near the ictal onset zone.

After the applying the artefact removal in patient 5 (see figure 6), 2 very tight clusters (depicted by the magenta ROI's in the dipole estimations of the filtered EEG) appeared, which did not correlate with the ictal SPECT. These clusters showed a very low relative residual energy, suggesting a high "goodness-of-fit". However, careful examination of the EEG during the ictal period showed in the unfiltered case that the signal was heavely distorted. Therefore, the neurologist had to remove a lot of components in the BSS-CCA procedure until the ictal activity became visible. A singular value decomposition of the ictal EEG after filtering showed that the EEG can be described by only 3 or 4 components. In that case, the topographies in the SVD decomposition remain fixed for a period of 10 seconds. As the EEG only consist of 3 topographies, the dipole estimations are very clustered. In BSS-CCA, the expert tries to remove all components that are due to muscle activity. For patient 5, the noise due to muscle activity was excessive, that the expert also removed the components corresponding to the ictal activity. This resulted in dipole estimations with a high "goodness-of-fit" but with no physiological meaning as the ictal content of the signal was changed by the artifact removal techniques.

From figures 4, 5, 6 and 7, we see clearly in patient 1, 3, 7 and 8 that removing the muscle and eye artifacts makes the dipole estimation more accurate. However, there are still some outliers and a perfect correlation between the dipole estimations and ictal SPECT is not obtained. This is due to the fact that source estimation depends on many paramters. One set of parameters is the head model. In the ideal case, the head model is are true representation of the head of the patient. In our study, the dataset did not contain individual MR images per patient. Thus a realistic head model from a standard T1 MR image was derived. Although the ictal SPECT can be coregistered with the MR image, the geometry of the head model plays an important role in the accuracy of the EEG source estimation. Moreover, the coregistration of the ictal SPECT image with an MR image, which did not originated from the patient, also introduces errors in the actual ictal SPECT location. The electrode

positions were placed according to the 10-20 system. An MR image of the patient with the electrodes on the scalp can be used to extract the electrode positions. In our study this was not the case. We projected the electrode positions from a sphere onto the scalp. The real electrode positions used in the measurement of the ictal activity, can deviate from the projected ones. These deviations can cause dipole estimation errors in the order of 1 cm if the average displacement of the electrode positions is 1 cm (Van Hoey et al., 2000). Besides electrode position displacement, uncertainty in conductivity values of the skull also causes considerable dipole localization errors. A deviation of the conductivity of the skull by a factor 2, can result in dipole location errors in the order of 1 to 2 cm (Vanrumste et al., 2000; Chen et al., 2007).

In figure 8 the median distance to the edge of the ictal SPECT is depicted for each patient in the filtered and unfiltered case. We clearly see that the dipole source estimation in patient 7 and 8 was improved by using the muscle and eye blink artifact removal. This is also clear from the dipole estimation in figure 7. The dipoles were estimated closer to the ictal SPECT activation. Qualitatively, patients 1 and 3 did show an improvement of the localization in the filtered case, however this was not reflected in the median. This was because the median is robust for outlier values and many dipole estimations in the unfiltered case were already close to the ictal SPECT. The median distance of patient 5 decreased in the unfiltered case, however, as mentioned before, this was due to too noisy data. The median in patient 2 and 6 did increase when the EEG was filtered using the BSS-CCA and SCICA. If the EEG is contaminated too much with muscle activity, many components have to be removed to make the underlying EEG visible. If too much components are removed by the neurologist, the measurement space will consist of few components. In some examples not shown here, EEG fragments of ten seconds consisted of only 4 or 5 SVD-components. If the remaining components represent the epileptogenic source, the estimated dipoles will be at the epileptogenic onset zone. Unfortunately, this is not always the case. Performing an estimation of the dipole source in a moving window with the RAP-MUSIC algorithm in such cases, could result in very clustered dipoles, with very low relative residual energy but with no physiological meaning. Thus, in cases of severe muscle contamination of the EEG carefull application of the BSS-CCA is advised. In EEGs moderately contaminated with muscle artifacts, however, BSS-CCA provides a more reliable estimation of the sources.

The muscle artifact removal was performed by the neurologist in 10 second windows. In each 10 second window components are removed until the neurologist could identify the EEG as muscle artifact free. However, the number of components removed differs from each 10 second window. This can result in abrupt changes of the signal-to-noise ratio at the 10 second window borders and thus in the dipole estimates location, which can be seen in figure 3. Future research will involve the automatic selection of components, so that the

abrupt changes in the dipole estimates can be resolved.

Finally, we want to point out the necessity of using a large number of electrodes to have a accurate dipole estimation. In our study we used a clinical setup of 21 electrode channels. In this case the brain activity and artifacts are captured in 21 channels. By using subspace techniques as a pre-processing step (BSS-CCA) and source estimation (RAP-MUSIC), subspaces have to be selected to remove the artifactuated components and/or construct the signal subspace. As seen in patient 5 (see figure 6), the removal of components in the pre-processing step limits the number of components available in the source estimation to construct the signal subspace. If only 21 channels are used, the neurologist can only choose between 21 sources. This can result that one source contains muscle activity as well as ictal activity. If a larger number of electrodes is used, the number of sources increases. This can yield a better separation between sources representing the muscle activity and source representing the ictal activity. Therefore, by using high resolution EEG (64 or 128 channels) a more accurate ellimination of the artefact and thus a more accurate estimation of the source can be carried out. However, this setup is less practical in the clinic.

6 Conclusion

The results show that the muscle and eye blink artefact removal techniques can improve the dipole estimation of ictal activity within an EEG fragment. The use of these techniques prior to the dipole source localization can provide a more reliable way of estimating the source of an epileptogenic focus.

However, some things are to be kept in mind. In EEGs moderately contaminated with muscle artifacts, however, BSS-CCA provides a more reliable estimation of the sources. In cases of severe muscle contamination of the EEG carefull application of the BSS-CCA is advised. Moreover, when the muscle artifact had a different spatial information as the spatial information of the epileptiform event, the expert did not remove many components using the BSS-CCA procedure. This resulted in tighter clusters near the ictal SPECT activation (seen in patient 1,2,6 and 7), but also some estimation errors due to residual muscle artifacts.

The removal of eye artifacts using SCICA proved to be useful in patients. The application of the artifact removal succesfully eliminated the dipole estimates which corresponded to the eye artifacts.

This is a pilot study involving patients with different types of epilepsy. Therefore, in the future, a thorough study with a large number of patients with

similar types of epilepsy will be performed.

References

Assaf, B. A., Ebersole, J. S., Oct 1997. Continuous source imaging of scalp ictal rhythms in temporal lobe epilepsy. Epilepsia 38 (10), 1114–1123.

Baillet, S., Mosher, J. C., Leahy, R. M., 2001. Electromagnetic brain mapping. IEEE Signal Processing Magazine November, 14–30.

Belouchrani, A., Abed-Meraim, K., Cardoso, J., Moulines, E., 1997. A blind source separation technique using second-order statistics. IEEE transactions on Signal Processing 45, 434–444.

Boon, P., D'Hav, M., Vanrumste, B., Hoey, G. V., Vonck, K., Walleghem, P. V., Caemaert, J., Achten, E., Reuck, J. D., Oct 2002. Ictal source localization in presurgical patients with refractory epilepsy. J Clin Neurophysiol 19 (5), 461–468.

Boon, P., Vandekerckhove, T., Achten, E., Thierry, E., Goossens, L., Vonck, K., D'have, M., Van Hoey, G., Vanrumste, B., Legros, B., Defreyne, L., De Reuck, J., December 1999. Epilepsy surgery in Belgium, the experience in Gent. Acta Neurologica Belgica 99 (4), 256–265.

Chen, F., Hallez, H., Van Hese, P., D'Asseler, Y., Lemahieu, I., 2007. Dipole estimation errors due to skull conductivity perturbations: simulation study in spherical head models. In: Proceedings of 2007 joint meeting of the 6th International Symposium on Noninvasive Functional Source Imaging of the Brain and Heart and the International Conference on Functional Biomedical Imaging. Hangzhou.

Choi, S., Cichocki, A., Park, H., Lee, S., 2005. Blind source separation and independent component analysis: a review. Neural Information Processing - Letters and Reviews 6(1), 1–57.

Comon, P., 1994. Independent component analysis, a new concept? Signal Processing 36 (3), 287–314.

De Clercq, W., Vergult, A., Vanrumste, B., Van Paesschen, W., Van Huffel, S., 2006. Canonical correlation analysis applied to remove muscle artifacts from the electroenceaphalogram. IEEE Transactions on Biomedical Engineering 53 (12), 2583–2587.

De Vos, M., De Lathauwer, L., Vergult, A., De Clercq, W., Van Paesschen, W., Van Huffel, S., 2006a. Jacobi iterations for spatially constrained independent component analysis. In: Proc. of the 7th international conference on methematics in signal processing (IMA 2007), Cirencester, England.

De Vos, M., De Lathauwer, L., Vergult, A., De Clercq, W., Van Paesschen, W., Van Huffel, S., December 2006b. Spatially constrained independent component analysis for real-time eye artifact removal from the electroencephalogram. In: Proc. of the first Annual Symposium of the IEEE/EMBS Benelux Chapter. (IEEE EMBS). pp. 159–163.

Ding, L., Worrell, G. A., Lagerlund, T. D., He, B., Aug 2006. 3d source localization of interictal spikes in epilepsy patients with mri lesions. Phys Med Biol 51 (16), 4047–4062.

Ferree, T., Eriksen, K., Tucker, D., Dec. 2000. Regional head tissue conductivity estimation for improved eeg analysis. Biomedical Engineering, IEEE Transactions on 47 (12), 1584–1592.

Friman, O., Borga, M., Lundberg, P., Knutsson, H., Jun 2002. Exploratory fmri analysis by autocorrelation maximization. Neuroimage 16 (2), 454–464.

Gonçalves, S., de Munck, J., Verbunt, J., Bijma, F., Heethaar, R., Lopes da Silva, F., June 2003. In vivo measurement of the brain and skull resistivities using an eit-based method and realistic models for the head. Biomedical Engineering, IEEE Transactions on 50 (6), 754–767.

Goncharova, I. I., McFarland, D. J., Vaughan, T. M., Wolpaw, J. R., Sep 2003. Emg contamination of eeg: spectral and topographical characteristics. Clinincal Neurophysiology 114 (9), 1580–1593.

Hallez, H., De Vos, M., Phlypo, R., Vanrumste, B., Van Hese, P., D'Asseler, Y., Van Paesschen, W., Van Huffel, S., Lemahieu, I., 2007. Can dipole modelling be improved by removing muscular and ocular artifacts from ictal scalp eeg? In: Proceedings of the 3rd international IEEE EMBS conference on Neural Engineering. pp. 252–255.

Hallez, H., Vanrumste, B., Van Hese, P., D'Asseler, Y., Lemahieu, I., Van de Walle, R., 2005. A finite difference method with reciprocity used to incorporate anisotropy in electroencephalogram dipole source localization. Physics in Medicine and Biology 50, 3787–3806.

Hotelling, H., 1936. Relations between two sets of variates. Biometrika 28, 321–377.

Joyce, C., Gorodnitsky, I., Kutas, M., 2004. Automatic removal of eye movement and blink artifacts from eeg data using blind component separation. Psychophysiology 41, 313–325.

Jung, T. P., Makeig, S., Humphries, C., Lee, T. W., McKeown, M. J., Iragui, V., Sejnowski, T. J., Mar 2000. Removing electroencephalographic artifacts by blind source separation. Psychophysiology 37 (2), 163–178.

Lantz, G., Michel, C. M., Seeck, M., Blanke, O., Landis, T., Rosn, I., Jan 1999. Frequency domain eeg source localization of ictal epileptiform activity in patients with partial complex epilepsy of temporal lobe origin. Clinical Neurophysiology 110 (1), 176–184.

Lee, S. K., Lee, S.-Y., Yun, C.-H., Lee, H.-Y., Lee, J.-S., Lee, D.-S., Sep 2006. Ictal spect in neocortical epilepsies: clinical usefulness and factors affecting the pattern of hyperperfusion. Neuroradiology 48 (9), 678–684.

Li, Y., Ma, Z., Lu, W., Li, Y., 2006. Automatic removal of the eye blink artifact from eeg using an ica-based template matching approach. Physiologic Measurements 27, 425–436.

Mosher, J. C., Leahy, R. M., 1999. Source localization using recursively applied and projected (rap) music. IEEE Transactions on Signal Processing 47, 332–340.

Nam, H., Yim, T.-G., Han, S. K., Oh, J.-B., Lee, S. K., Feb 2002. Independent component analysis of ictal eeg in medial temporal lobe epilepsy. Epilepsia 43 (2), 160–164.

Niedermeyer, E., Lopez Da Silva, F., 2004. Electroencephalography: Basic Principles, Clinical Applications, and Related Fields, 5th Edition. Lippincott Williams & Wilkins.

Sakai, Y., Nagano, H., Sakata, A., Kinoshita, S., Hamasaki, N., Shima, F., Morioka, T., Apr 2002. Localization of epileptogenic zone in temporal lobe epilepsy by ictal scalp eeg. Seizure 11 (3), 163–168.

Shoker, L., Sanei, S., Wang, W., Chambers, J. A., Mar 2005. Removal of eye blinking artifact from the electro-encephalogram, incorporating a new constrained blind source separation algorithm. Med Biol Eng Comput 43 (2), 290–295.

Stern, J. M., Engel, J., 2004. Atlas of EEG patterns. Lippincott, Williams & Wilkins.

Van Hoey, G., B., V., D'Havé, M., Van de Walle, R., Lemahieu, I., Boon, P., 2000. Influence of measurement noise and electrode mislocation on eeg dipole-source localisation. Medical & Biological Engineering & Computing 38, 287–296.

Van Paesschen, W., 2004. Ictal spect. Epilepsia 45 Suppl 4, 35–40.

Vanrumste, B., Van Hoey, G., Van de Walle, R., D'Have, M., Lemahieu, I., Boon, P., 2000. Dipole location errors in electroencephalogram source analysis due to volume conductor model errors. Medical & Biological Engineering & Computing 38, 528–534.

Figures

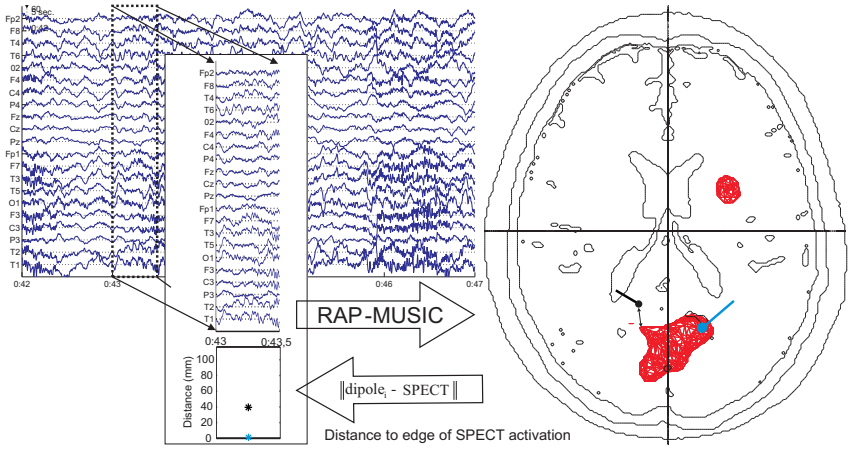
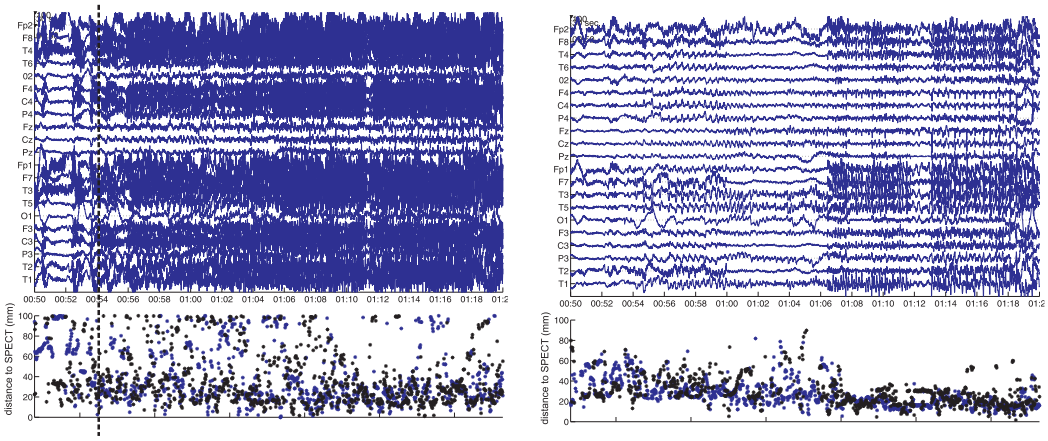
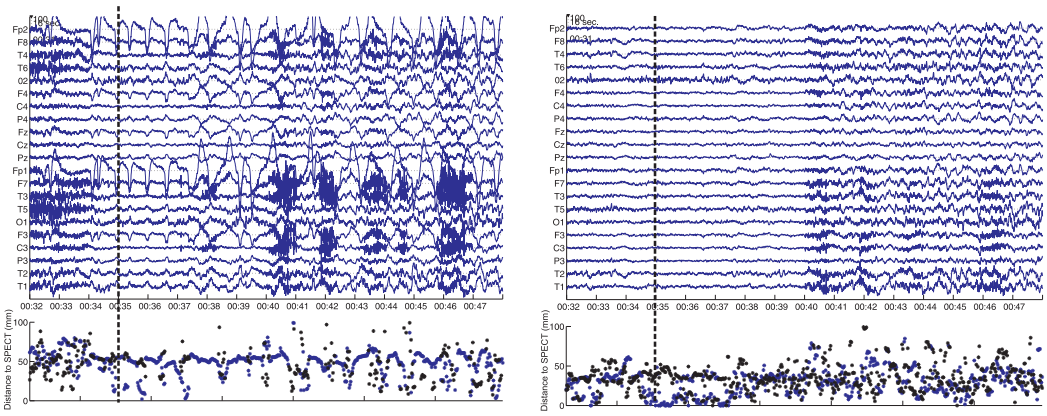


Fig. 1. A schematic of the calculation of the distance between the dipole locations and the edge of the 95% surface of the ictal SPECT activation. In a moving window of 62 samples ($\approx$ 0.2 sec) a maximum of 2 dipoles are estimated using the RAP–MUSIC algorithm. The distance of each dipole to the edge of the 95% interval of the ictal SPECT activation is then calculated and put in a seperate figure.



(a) (b)

Fig. 2. In this figure we can see an EEG fragment of 30 seconds in (a) the unfiltered case and (b) the filtered case. Below the EEG fragements the distance measure (in mm) is shown. The seizure start as indicated by the neurologist was between 53 and 54 seconds. In the unfiltered EEG, we can see that the distance from the dipole to the ictal SPECT activation is very high ($\geq$ 100 mm) and is very irregular. The black asterisk and bleu asterisk indicate the distance of the first and second dipole to the ictal SPECT activation, respectively.



(a) (b)

Fig. 3. Figure (a) and (b) show the distance of the dipoles to the center of gravity of the ictal SPECT activation for the unfiltered and filtered EEG respectively in function of time. The results show an EEG window of 14 seconds en below the distance measure (in mm). The seizure start, as indicated by the neurologist, was at 35 seconds. In the unfiltered EEG, we can see that the distance from the dipole to the ictal SPECT activation is very high due to eye artifacts. In the filtered EEG, the dipoles from the early seizure onset are situated in or near the SPECT activation. The black asterisk and bleu asterisk indicate the distance of the first and second dipole to the ictal SPECT activation, respectively.

Tables

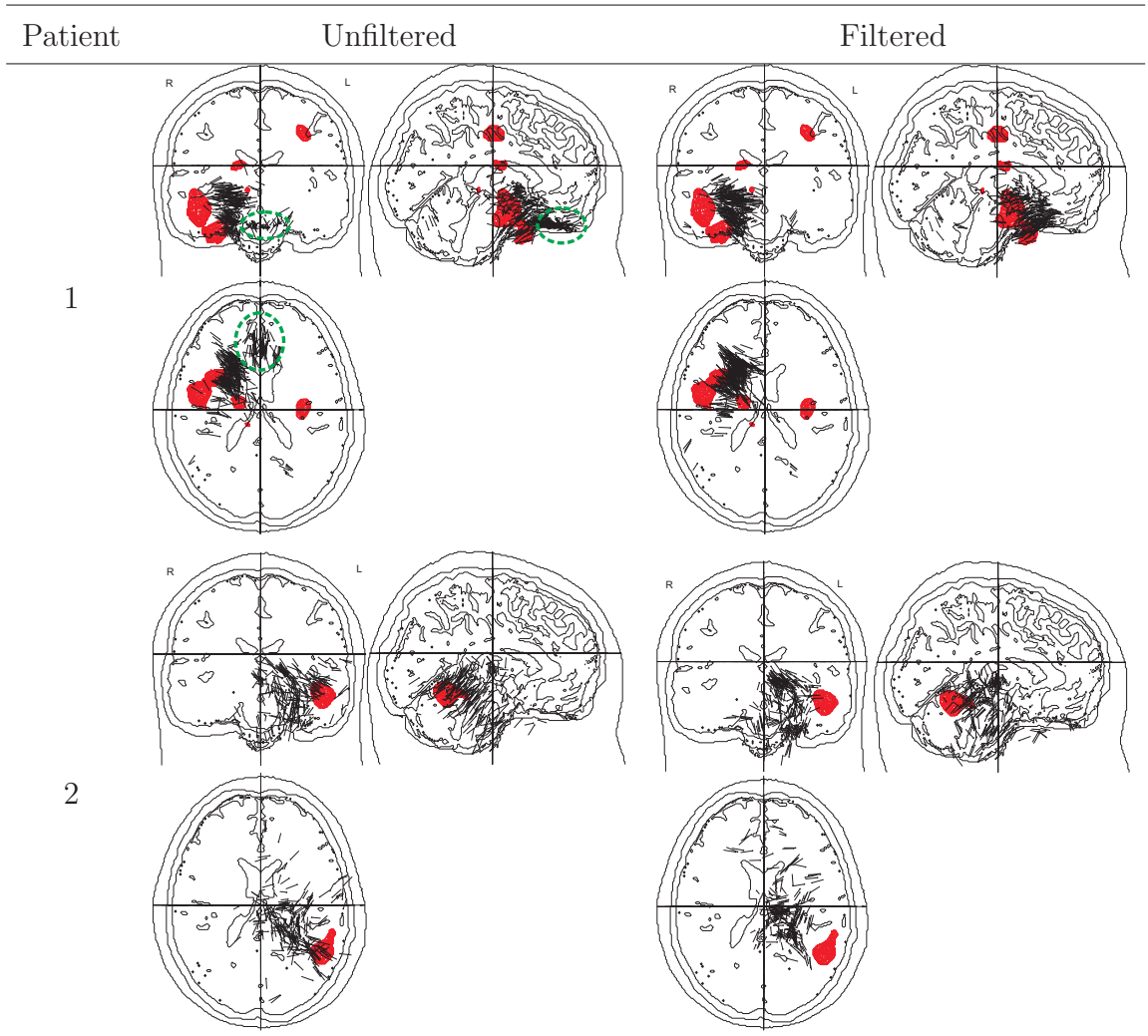


Fig. 4. Patient 1 and 2: The dipole estimations during a 21 second interval starting one second prior to the start of the seizure in the case of the unfiltered EEG data (left) and filtered EEG data (right). Each figure depicts 3 views of the dipole estimations in the realistic head model: axial, sagital and coronal. The red contour denote the thresholded ictal spect activity coregistered with the realistic head model. For the sake of visualization, the threshold of the ictal spect was chosen to be 85% instead of the 95% used in the calculations (a 95% surface resulted in a very small area, which could be obscured by the dipole estimations). In patient 1 the green circle indicates a region of interest depicting the dipole estimations during an eye blink artefact. This results in dipole estimations estimated very near the eyes.

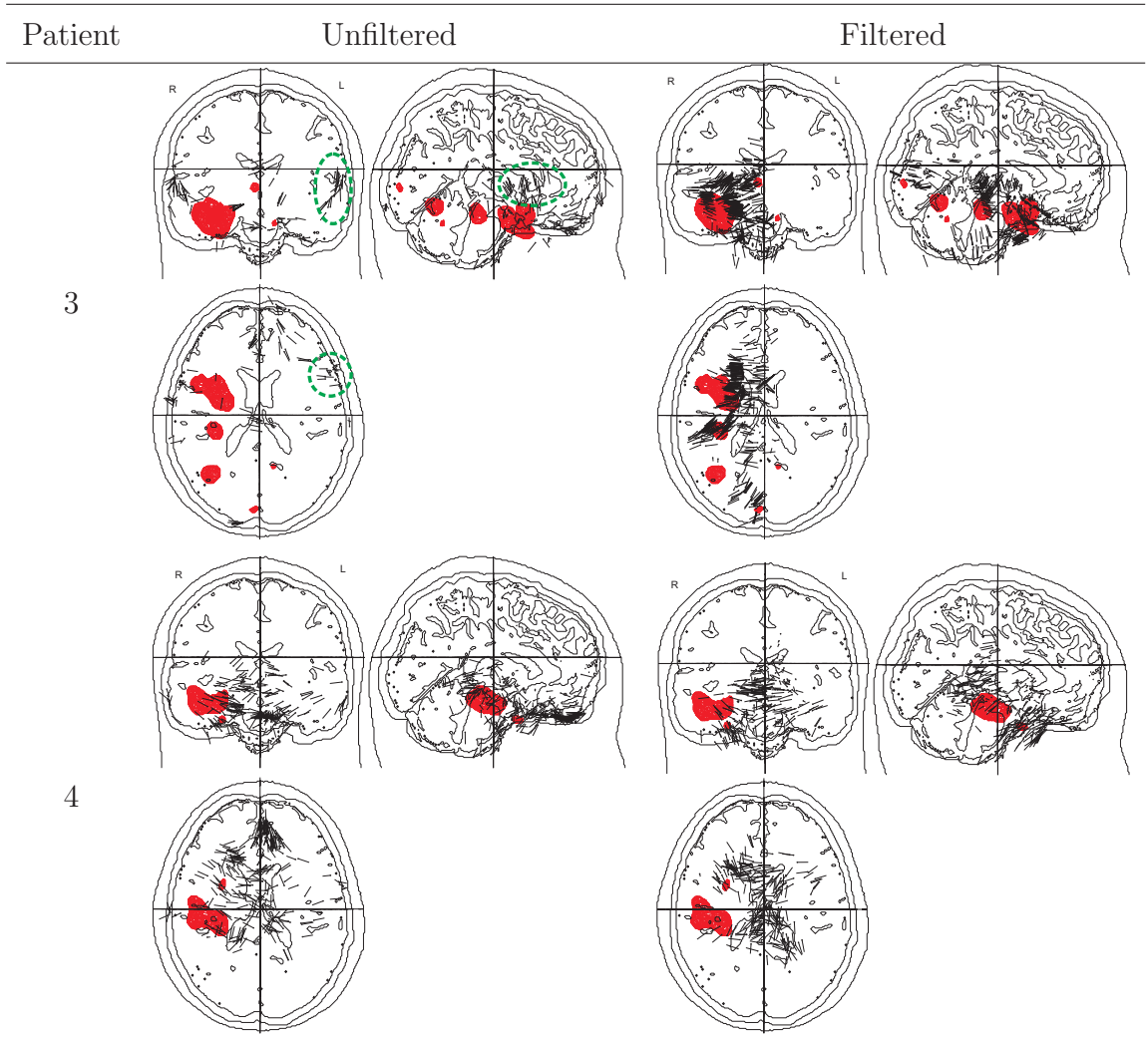


Fig. 5. Figure 4 continuted. Patient 3 and 4: The dipole estimations during a 21 second interval starting one second prior to the start of the seizure in the case of the unfiltered EEG data (left) and filtered EEG data (right). Each figure depicts 3 views of the dipole estimations in the realistic head model: axial, sagital and coronal. The red contour denote the thresholded ictal spect activity coregistered with the realistic head model. In patient 3 the green circle indicates a region of interest depicting the dipole estimations due to the muscle activity. This results in dipole estimations estimated very near to muscle.

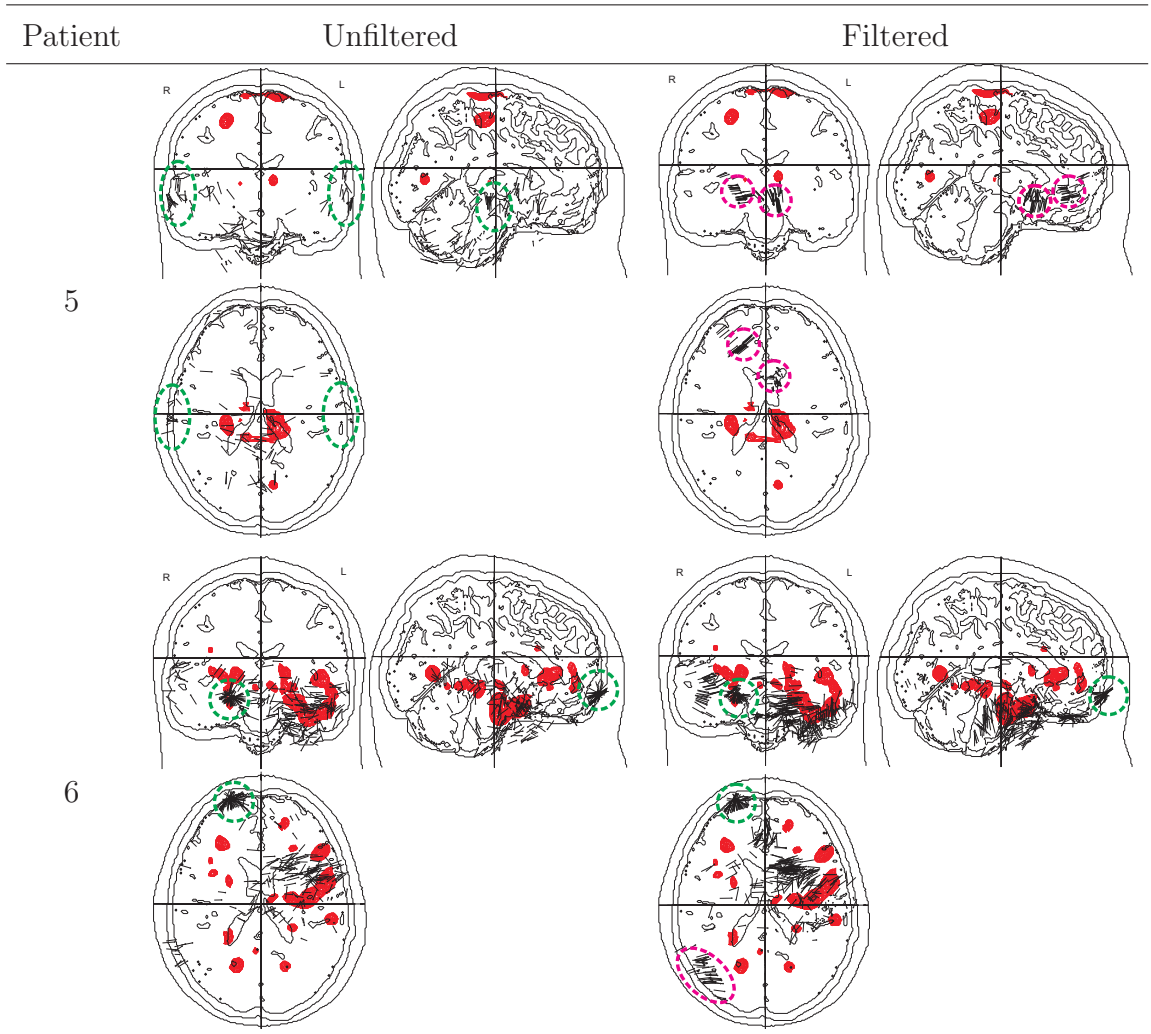


Fig. 6. Figure 4 continuted. Patient 5 and 6: The dipole estimations during a 21 second interval starting one second prior to the start of the seizure in the case of the unfiltered EEG data (left) and filtered EEG data (right). Each figure depicts 3 views of the dipole estimations in the realistic head model: axial, sagital and coronal. The red contour denote the thresholded ictal spect activity coregistered with the realistic head model. For the sake of visualization, the threshold of the ictal spect was chosen to be 85% instead of the 95% used in the calculations. In patient 5 the green circle indicates a region of interest depicting the dipole estimations due to the muscle activity. This results in dipole estimations estimated very near to muscle. The magenta circle in patient 5 indicates the 2 very tight clusters after artefact removal was applied. In patient 6 the green ROI indicates the dipoles due to the electrode artefact at one of the frontal electrodes.

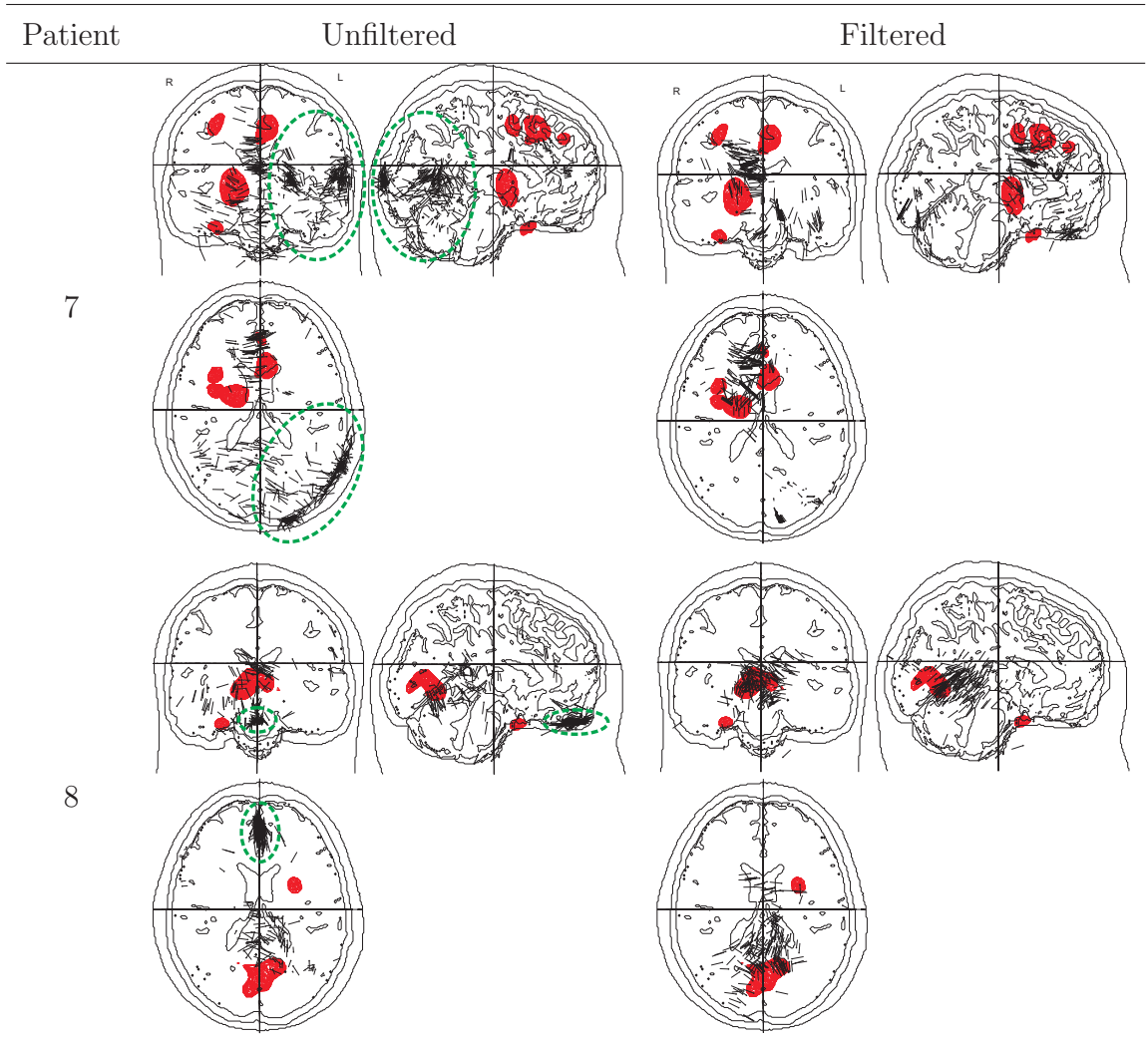


Fig. 7. Figure 4 continuted. Patient 7 and 8: The dipole estimations during a 21 second interval starting one second prior to the start of the seizure in the case of the unfiltered EEG data (left) and filtered EEG data (right). Each figure depicts 3 views of the dipole estimations in the realistic head model: axial, sagital and coronal. The red contour denote the thresholded ictal spect activity coregistered with the realistic head model. In patient 7 the green circle indicates a region of interest which depicts the dipole estimation due to muscle activity. In patient 8 the green ROI depicts the dipoles during source analysis during eye blink artefacts.

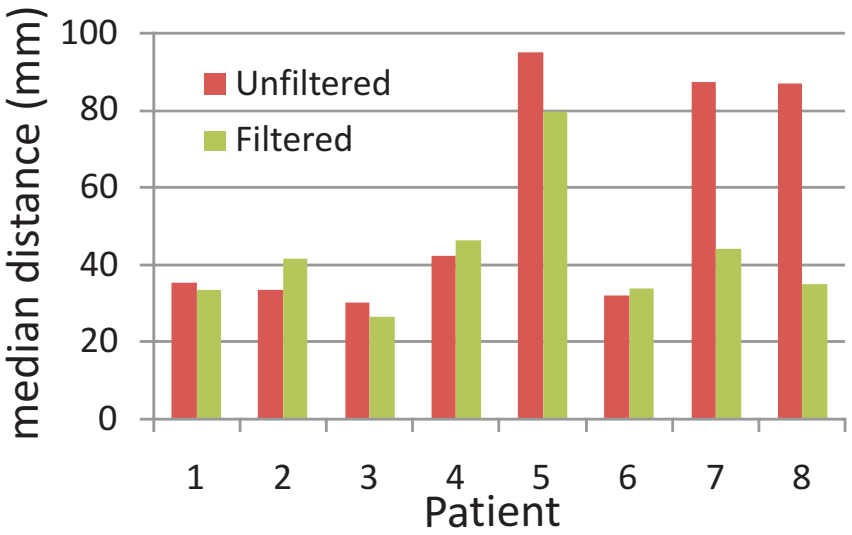


Fig. 8. The median distance between the dipole locations and the edge of the iS-PECT activation for the filtered (in red) and unfiltered (in green) case for all 8 patients.

Table 1
The patient data used in the study. Gender: M = Male, F = Female. Frequency CPS = frequency of complex partial seizures per month. MRI: HS = Hippocampal sclerosis, Nl = Normal, CD = cortical dysplasie, PS = Posttraumatic scar. EEG localization and SISCOM: L = left, R = right, T = temporal, F = frontal, C = central, O = occipital, NA = not applicable. Engel outcome Scores: I = seizure free, II = almost seizure free, III = 75% seizure reduction, IV = no improvement. Duration of seizure is in seconds and time of injection is in seconds after the seizure onset.

Patient	Age	Gender	Age at onset	FrCPS	MRI MRI	Latera-lization	Ictal EEG Ictal EEG	duration of seizure	time of injection	SISCOM SISCOM	surgery performed	Engel outcome
1	32	M	4	5	HS	L	LT	67	27	LT	Yes	I
2	59	M	39	20	Nl	R	RT	96	17	RT	Yes	II
3	35	F	25	15	HS	L	LT	94	12	LT	Yes	I
4	36	F	15	4	Nl	L	LFT	33	17	LT	No	NA
5	20	F	2	30	Nl	L	NA	93	25	LP	No	NA
6	30	M	6	8	CD	L	FC	70	18	LF	Yes	I
7	38	F	5	4	PS	L	LFC	36	3	LFT	No	NA
8	41	F	20	10	Nl	R	O	160	26	O	No	NA